THE AMERICAN SOCIETY OF MECHANICAL ENGINEERS
345 E. 47th St., New York, N.Y. 10017

97-GT-386

EFFECTS OF ENGINE AGING ON AIRCRAFT NO_x EMISSIONS

Stephen P. Lukachko and Ian A. Waitz
Massachusetts Institute of Technology
Aero-Environmental Research Laboratory
77 Massachusetts Avenue, Building 31-269
Cambridge, MA 02139

ABSTRACT

The impact of representative paths of engine degradation on aircraft cruise NO_x emissions was investigated. Engine cycles corresponding to older, current, and future subsonic and supersonic technologies were developed and used to determine the sensitivities of combustor conditions to various changes in component efficiencies and flow capacities due to aging. Estimates of relative changes in NO_x emissions levels were made using established empirical correlations that relate emissions to combustor flow parameters. The analysis methodology was validated through comparisons to test data where available.

It was found that the sensitivity of specific fuel consumption (SFC) and combustor flow parameters to component aging is enhanced by increases in cycle temperatures and pressures. This ultimately results in a higher sensitivity of NO_x emissions to engine degradation for cycles representative of more advanced technology. At constant thrust, turbine degradation typically acts to decrease NO_x emissions while compressor aging results in an increase in NO_x emissions; both occurring at the expense of SFC. Sample degradation scenarios were used to highlight the balance between turbine and compressor aging effects. Changes in NO_x emissions in the -1% to +4% range were predicted for typical aging scenarios. The applicability of these results to the formulation of aircraft emissions inventories is considered.

NOMENCLATURE

EGT	exhaust gas temperature (K)
$EINO_x$	emission index (g NO_x (as NO_2) / kg fuel burned)
EPR	engine pressure ratio (P_{T5}/P_{T2})
FF	fuel flow rate (kg/s)
N1,N2	low, high pressure spool speeds (rpm)
OPR	overall pressure ratio (P_{T3}/P_{T2})
P	pressure (Pa)
P_{comb}	combustion chamber pressure (Pa)
P_T	stagnation pressure (Pa)
SFC	specific fuel consumption (kg/kN)
t_{res}	combustor residence time (s)
T	temperature (K)
T_{adiab}	adiabatic flame temperature (K)
T_T	stagnation temperature (K)

Subscripts

2	fan inlet
3	compressor exit/combustor inlet
4	combustor exit/turbine inlet
5	low-pressure turbine exit

1. OBJECTIVE AND APPROACH

Several programs of research initiated within the last decade in both the United States and Europe focus on understanding the ozone and climate impacts of supersonic and, more recently, subsonic aircraft emissions (NASA-ICAO, 1996). Oxides of nitrogen (NO_x) emissions continue to be the primary foci of environmental concern with regards to the atmosphere because of their potential effects on ozone concentrations in both the troposphere and the stratosphere. The development of global emissions inventories, *in situ* exhaust sampling campaigns, ground level engine tests, and modeling efforts organized to characterize the exhaust composition of both individual engines and global fleets are central components to these assessment efforts.

The objective of this study was to determine the effect of engine aging on NO_x emissions and thus to determine the extent of the uncertainty introduced by engine aging in emissions databases. A second goal was to examine how these effects change as gas turbine technology evolves.

Presented at the International Gas Turbine & Aeroengine Congress & Exhibition
Orlando, Florida — June 2–5, 1997

Because of the expense and length of time required to complete exhaust characterization tests, it is important to enumerate and classify sources of uncertainty that may complicate the interpretation of results. One basic uncertainty that affects all characterization data is the change in exhaust speciation due to the effects of aging on engine operation. However, an account of these effects is usually not undertaken. For example, in the International Civil Aviation Organization Engine Exhaust Emissions Data Bank (ICAO, 1995), which is the primary source of input for global atmospheric models used to predict the effects of aircraft on the atmosphere, the majority of data reported is based on tests conducted using new production engines or dedicated test engines. No systematic account of the effects of engine age or maintenance practice is provided. With an understanding of the effects of engine aging on aircraft NO_x emissions, scientific assessments of aircraft emissions can move to address the consequences of uncertainty in exhaust characterization and ultimately, any subsequent effects on the results of global atmospheric modeling.

The only publicly available study of the effects of engine aging on carbon monoxide (CO), hydrocarbons (HC), and NO_x emissions was performed in the early 1970's to support the formulation of early emissions certification requirements (Platt and Norster, 1978; Platt and Norster, 1979). Efforts to understand variability in engine emissions due to maintenance procedures were also conducted (Becker *et al*., 1980; Frings, 1980). The results of these studies are discussed in greater detail in Section 2. Despite the importance of these studies, no publicly reported effort to broaden and update this limited empirical database has been undertaken.

In lieu of an adequate empirical database from which to work, a modeling approach was employed in this study to provide some insight into the effects of engine aging on NO_x emissions. Representative cycles corresponding to older, current, and future subsonic and supersonic technologies were developed. These cycles were used to determine the sensitivities of combustor flow conditions to various changes in component efficiencies and flow capacity that typically result from engine aging. Focus was given to the cruise condition. The resulting changes in NO_x emissions levels were determined using established empirical correlations that relate emissions to combustor flow conditions. This analysis methodology was validated through comparisons to test data where available.

To set the context for discussion of the effects of engine deterioration on NO_x emissions, Section 2 provides an overview of the existing data on overall engine performance and emissions change with aging, as well as emissions variability for both new and maintained engines. Methods for correlating engine deterioration with changes in performance parameters and practical limits to losses incurred before overhaul are also presented. Section 3 discusses the research methodology employed in the current study, including the development and validation of representative engine cycles, methods for correlating changes in performance parameters with changes in NO_x emissions levels, and the models and scenarios for engine aging employed. Section 4 presents and discusses results for sensitivity to component deterioration, technological trends, and results for representative scenario calculations. Section 5 contains a discussion of the importance of these results with regard to the accuracy of emissions databases. Section 6 closes the paper with a summary and suggestions for future research.

2. OVERVIEW OF ENGINE AGING, MAINTENANCE, AND OPERATIONAL VARIABILITY

There are several contexts in which to consider the effects of aging on engine operation. Knowledge of aging effects is important for monitoring the health and diagnosing the maintenance needs of gas turbine engines, for the development of flight deck instrumentation that conveys the correct state of engine operation, and for the development of regulatory certification requirements for aircraft engines with respect to various exhaust constituents. Deciphering the modes of component degradation and failure through measurements of key engine parameters is basic to the conduct of all of these activities. These engine parameters determine emissions levels both directly and indirectly.

2.1 Engine Aging

Engine deterioration can be characterized as the summation of short-term and long-term effects, both of which result in performance losses. These trends are shown schematically in Figure 1 taken from Wulf (1980). Typically, a rapid loss occurs during the engine's initial service flight followed by a gradual performance degradation until the engine is refurbished. For both economic and mechanical reasons, only part of this total degradation is restored in the maintenance process resulting in an engine returned to service with a reduced level of performance. As the engine continues operation, these unrecovered losses increase with additional maintenance cycles. A portion of the long term losses are cyclically restored with each repair.

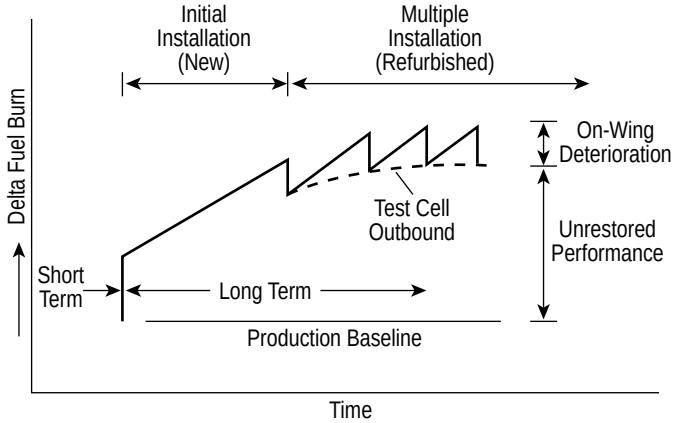

Figure 1: A model of engine deterioration. [Adapted from Wulf (1980), Fig. 3.1]

For the GE CF6-50 engine, Wulf (1980) found that short-term deterioration was more closely associated with the engine design itself rather than the operational use of the engine. Long-term losses were more related to the operational characteristics of the aircraft employing the engine and therefore were more appropriately correlated with the fleet rather than the engine. Other studies indicate that for some individual components, degradation is correlated with number of cycles rather than hours in use (Richardson *et al*., 1979).

As a practical matter, tracing the degradation of an engine to its cause is a difficult prospect. Engine performance deterioration is associated with several aging conditions that are of a time-developing nature. These include physical distortion of engine parts due to corrosion, the ingestion of foreign objects, the buildup of deposits (fouling), erosion of parts, and general wear. Degradation is empirically manifest as changes in measurable engine parameters such as exhaust gas temperature (EGT), fuel consumption (as specific fuel consumption, SFC, or fuel flow, FF), turbine inlet temperature (T_{T4}), low or high pressure spool speeds (N1 or N2 respectively), and/or engine pressure ratio (EPR), as well as changes in engine performance bounds such as the stall margin. Methods used to investigate mechanical performance include vibrational analyses and oil consumption tests. A key difficulty lies in associating a specific condition or combination of problems with measured performance parameters. Because this capability is important for bounding the changes in NO_x that might reasonably be expected, Section 2.2 details research conducted on this issue.

2.2 Methods for Correlating Aging with Changes in Performance Parameters

Before the introduction of analytically oriented techniques, engine degradation was understood through empirically developed relationships between engine parameters and degradation effects as revealed through inspection and, eventually, through in-flight or ground testing performance data (Arnold and Gast, 1970; Treager, 1979). Trend plots were used to map the deviation of engine parameters from a manufacturer specified baseline to better recognize the existence of a fault. However, this type of analysis generally did not provide enough information to specify what composed the fault (Aker and Saravanamuttoo, 1989).

More analytically driven studies geared towards prediction of fault occurrences and levels of degradation led to the development of methods based on an understanding of engine cycles. Urban (1974) proposed a linear analysis method where measurable parameter changes are associated with changes in the performance characteristics of engine components using fundamental performance equations specific to a particular engine. Recognizing limitations in the trend plotting and linear analysis approaches, Saravanamuttoo and MacIsaac (1983) proposed a nonlinear methodology based on cycle deck analysis to be used in concert with trend analyses. Like Urban, Saravanamuttoo and MacIsaac proposed to show changes in critical engine parameters through correlation with changes in measurable parameters. They also suggested that with the use of cycle decks employing generic component performance maps, degradation could be associated with particular problems through the use of fault matrices. Using fault matrices, cycle deck modeling results were typically presented as a grid of faults associated with qualitative (*e.g.* visual representations of increases or decreases in measurable parameters) rather than quantitative trends in measurable engine parameters. Early use of fault matrices employed assumptions about the effects of a fault in terms of component efficiencies and flow capacities without empirical verification (MacIssac, 1992). Importantly, Saravanamuttoo and MacIsaac showed that engine models could be employed as a predictive rather than a solely diagnostic tool using models of faults constructed as combinations of efficiency and flow capacity changes. A similar approach was employed in the current study. Cycle deck calculations with generic component maps were used and engine degradation was modeled via changes in flow capacity and efficiency.

In response to the lack of rigorous connection with actual deterioration circumstances, recent efforts have concentrated on developing models of specific faults that can be verified, primarily for the case of compressor fouling. Although the intention of the current study is to provide only a representative analysis of the effects of component degradation on emissions, more quantitative analysis associated with specific faults can be developed. Using the methods reviewed above, several authors have attempted to model or show the effects of various types of degradation on engine performance (Saravanamutto and MacIsaac, 1983; Saravanamuttoo and Lakshminarasimha, 1985; Lakshminarasimha and Saravanamuttoo, 1986; Dupuis *et al.*, 1986; Aker and Saravanamuttoo, 1989). Among these, Dupuis *et al.* conclude that the superposition of individual component fault effects on an engine can suffice for a multiple component fault simulation with a high degree of accuracy. Papers within the last few years have given more detailed accounts of individual fault effects (Stevensen and Saravanamuttoo, 1995; Singh *et al.*, 1996).

2.3 Maintenance Practice and Restoration of Losses

Aircraft engines traditionally have been maintained according to a manufacturer suggested schedule tempered by inspection of the engine before maintenance by the operator and in a manner approved by the Federal Aviation Administration (FAA) (Treager, 1979). In aircraft applications, maintenance practices are usually predicated on thresholds of allowable engine degradation determined by economic considerations which can be understood as a balance between the cost of inefficient aircraft operation and maintenance expenditures, and safety concerns which exist as more absolute bounds on allowable deterioration. This method of performing maintenance only when needed, known as *on-condition* maintenance, requires a close monitoring of measurable engine parameters as well as detailed inspections of engine components during scheduled visits, taking advantage of further opportunities for inspection when they arise.

There has been little reported research on the effectiveness of maintenance procedures in correcting faults and restoring losses. Proprietary concerns of aircraft engine manufacturers limit the disclosure of such competitive information. Engine overhauls may cost as much as $1M for a single engine and all losses may not be recovered in the maintenance cycle while the engine remains usable for service. For example, Wulf (1980) found that it was economical to restore only 70% of long-term unrestored losses.

Despite a lack of data, representative limits of the extent to which engines may degrade can be established. For example, Urban (1974) suggests typical limits on changes in engine parameters and reasons for their existence for a dual-spool turbofan engine, as shown in Table 1.

Table 1: Typical Limits on Changes in Engine Parameters for a Turbofan Engine
[Adapted from Urban (1974), Fig. 14, p. 19-14]

Parameter	Limit	Reason
Fan mass flow	-5.0%	LPC surge
LPC mass flow	-8.0%	High turbine temp.
Fan efficiency	-5.0%	High turbine temp.
HPC mass flow	-8.0%	High RPM
HPC efficiency	-4.5%	High turbine temp.
HPT nozzle effective area	6.0%	LPC surge
HPT nozzle effective area	-6.0%	HPC surge
HPT efficiency	-5.0%	High turbine temp.
LPT nozzle effective area	8.0%	Low thrust
LPT nozzle effective area	-6.0%	LPC surge
Combustor exit temp.	2.5%	Turbine life
Specific fuel consumption	4.0%	Economy

Typically, component efficiency losses and flow capacity changes result in hotter cycle temperatures indicated by a rise in EGT. An overhaul condition is roughly suggested by a rise in EGT between 30 - 50 K and/or an increase in SFC of between 2 - 4 % (Urban, 1974; Treager, 1979; Frith, 1993). Given this data, we have chosen to use a 3% increase in the SFC as a reasonable degradation limit with which to investigate the effects of engine aging on NO_x emissions.

2.4 Sources and Extent of Engine Emissions Variability

There are many sources of engine emissions variability, including manufacturing differences in new engines, different aging characteristics for individual engines, and changes in fuel content, atmospheric conditions, or operational use. Extracting a trend that would suggest changes in emissions over a period of time must be undertaken amidst the uncertainty associated with these various factors. There have been a limited number of studies considering the variability of emissions in new engines and the effects of maintenance on overall emissions levels. Table 2 summarizes published data regarding emissions variability. Although not always undertaken, corrections are usually made for differences in ambient conditions and, where possible, for changes in fuel content, in order for the data to be comparable. However, Lyon, Dodds, and Bahr (1980) found that the variability of NO_x emissions was only slightly influenced by fuel type, fuel content, or sampling methods. Despite the lack of consistency in methodologies and reported units among the studies summarized in Table 2, the data provides some indication of the expected magnitudes of variability. The typical standard deviation for the data in Table 2 is 5-6% in the NO_x emissions index ($EINO_x = gNO_x$ (as NO_2)/ kg fuel burned) for the power settings closest to the cruise condition, but there is a wide range represented in the data.

Also shown in Table 2 are measurements obtained immediately after maintenance has been performed. In particular, Becker *et al.* (1980) investigated the exhaust characteristics of a sample of seven JT8D-7A gas turbines after overhaul finding that properly overhauled engines should have emissions levels and variability similar to new engines. Standard deviations for NO_x emissions ranged from 7.1% at 100% rated takeoff power to 40.7% at idle. Collectively, these data combine to give a standard deviation of 14.5% in the NO_x EPA parameter (EPAP). Becker *et al.* also present data on variability among new production engines in graphical form indicating an approximately 23.5% standard deviation in the NO_x EPAP for a much larger sample of newly manufactured engines. An earlier test of the CF6-50 conducted by Frings (1980) showed a 2.8% standard deviation in the NO_x EPAP emissions level among a sample of engines tested after undergoing various levels of maintenance.

The emissions certification process also provides some insight into expected levels of variability in engines. Studies on engine variability (*e.g.* Table 2) were incorporated into the formulation of emissions certification procedures for newly manufactured engines because verification of compliance was a central issue in the promulgation of emissions requirements (43 FR 58, 1978; 47 FR 251, 1982; 55 FR 155, 1990; ICAO, 1993). These procedures are based on a composite distribution of historical engine to engine variability and imply that the NO_x emissions measured for a single engine test would be expected fall within an interval equivalent to 31.8% of the mean NO_x kg/kN (*e.g.* Dp/ Foo or EPAP) test result with 90% confidence.

Comparisons of emissions *variability* between maintained engines and new engines (*e.g.* Becker *et al.*, 1980; Frings, 1980) do not directly address changes in the *average* emissions levels that occur as a result of engine aging. It is this point which is of primary interest for the current study. Only one report found by the authors addresses this issue. Platt and Norster (1979) published emissions degradation factors per 1000 hours of engine use in terms of EIs and EPAPs for NO, CO, and HC. A summary of the Platt and Norster results is given in Table 3 for the engines tested. No results for the cruise condition were presented.

The data in Table 3, using a constant thrust power setting, indicate a *decrease* in NO emissions as a function engine age,

Table 2: New and Maintained Engine Emissions Variability

Engine Type	Engine Condition	Tests	Setting [6]	Std. Deviation [7]	Corrections
CF6-50C2 [1a]	new, post checkout	6	30% rO	6.5-6.9% $EINO_x$	P3, T3, H, FF
CF6-50C2 [1b]	new, post checkout	12	30% rO	4.8-4.9% $EINO_x$	P3, T3, H, FF
CF6-6 [1a]	new, post checkout	7	30% rO	4.0-4.2% $EINO_x$	P3, T3, H, FF
CF6-50C2 [1a]	new, post checkout	6	85% rO	1.4-2.6% $EINO_x$	P3, T3, H, FF
CF6-50C2 [1b]	new, post checkout	12	85% rO	5.7-6.2% $EINO_x$	P3, T3, H, FF
CF6-6 [1a]	new, post checkout	7	85% rO	2.5-3.3% $EINO_x$	P3, T3, H, FF
CF6-50C2 [1a]	new, post checkout	6	LTO cycle	0.9-1.5% EPAP	P3, T3, H, FF
CF6-50C2 [1b]	new, post checkout	12	LTO cycle	4.9-5.0% EPAP	P3, T3, H, FF
CF6-6 [1a]	new, post checkout	7	LTO cycle	3.4-4.0% EPAP	P3, T3, H, FF
JT8D-7A [2]	post on-cond. maint.	7	30% rO	23.6% lb/hr	not reported
JT8D-7A [2]	post on-cond. maint.	7	85% rO	10.7% lb/hr	not reported
JT8D-7A [2]	post on-cond. maint.	7	LTO cycle	14.5% EPAP	not reported
JT8D-7A [2]	newly manufactured	7	LTO cycle	23.5% EPAP	not reported
CF6-50 [3]	4 on-cond. maint., 1 no maint.	5	LTO cycle	2.81% EPAP	not reported
CF6-50 [4]	factory engine for development tests	1	30% rO	3.7% EINOx	not reported
CF6-50 [4]	factory engine for development tests	1	85% rO	4.5% EINOx	not reported
CF6-50C2 [5]	newly manufactured	6	LTO cycle	0.81% Dp/Foo	ambient effects
CF6-50 [5]	newly manufactured	6	LTO cycle	0.83% Dp/Foo	ambient effects
GE90-85B[5]	newly manufactured	3	LTO cycle	1.97-3.72% Dp/Foo	ambient effects
Olympus 593 Mk 610 [5]	newly manufactured	6	LTO cycle	5.7% Dp/Foo	ambient effects

Notes and Sources:

[1a] Source: Lyon, Dodds, and Bahr (1980). Using Jet A fuel. 'P3, T3, H, FF' = correction to combustor inlet conditions and ambient humidity, as well as a fuel flow correction used.

[1b] Source: Lyon, Dodds, and Bahr (1980). Using JP-4 fuel.

[2] Source: Becker, Frings, and Cavage (1980). All data as wet NO_x.

[3] Source: Frings (1981). Data as wet NO_x.

[4] Source: Lyon and Bahr (1981). Developmental combustor used in engine.

[5] Source: ICAO Engine Exhaust Emissions Data Bank (1995). Tests for CF6-50C2 and CF6-50 Oct.-Dec. 1979; for GE90-85B, Feb.-July 1995; for Olympus, Jun 1974-Nov. 1977. 'Ambient effects' = correction to ambient pressure, temperature, humidity.

[6] rO = rated output; LTO cycle = landing take-off cycle.

[7] EPAP = lbs pollutant / 1000 lbs thrust / LTO cycle; Dp/Foo = kg pollutant / kN rated thrust / LTO cycle. The EPA parameter (EPAP) is a measure of the total emissions of an aircraft engine over a typical landing-take-off (LTO) cycle. For NO_x, the EPAP is given in units of lbs of NO_x (as NO_2) per 1000 lbs of engine rated thrust output (rO) per LTO cycle. The LTO cycle is defined by a schedule of operating times in five particular modes; taxi/idle (79% of total LTO), takeoff (2%), climb out (7%), approach (12%). The tests are performed at thrust settings specified as %rO corresponding to the various modes. They are 30%, 100%, and 85% respectively. Emissions test results are weighted by the times-in-mode to provide a summation used for the EPAP calculation. The EPAP is equivalent the Dp/Foo parameter of ICAO international standards which is given as kg pollutant per kN rated thrust per LTO cycle. Note that the LTO cycle and thrust settings are different for supersonic and turboprop aircraft.

with the exception of the increase shown for the RB211 engine. Platt and Norster (1979) addressed the reason for this perhaps counter-intuitive trend explaining that, "significant deterioration of the turbine stator vanes would cause the operating line of the engine to move away from the surge line, resulting in an increased velocity through the combustor and less time for NO formation." Thus, the reduction in NO was associated with an increase in mass flow due to hot section damage. Indeed, as will be shown later in this paper, turbine damage is expected to result in a lower NO_x emissions rate. The RB211 result of increased emissions with age was attributed to increased operating temperatures rather than reduced residence time, which would be consistent with compressor deterioration as discussed in Section 4.

3. RESEARCH METHODOLOGY

Having considered the available information on maintenance practice, new and maintained engine emissions variability, and performance changes resulting from deterioration, the rest of the paper deals more directly with the execution of the present study. The following three sections discuss the development and validation of the representative cycles used to simulate deterioration (3.1), methods for correlating engine performance with emissions levels (3.2), and the application of these correlative methods in the study (3.3).

3.1 Development and Validation of Representative Engine Cycles

Four different engine cycles were developed for use in this study. Three cycles represent subsonic technologies and the fourth cycle represents one possibility for a future supersonic transport engine design. The CF6-50C2 was used as an example of older in-use technology and a cycle modeled after the GE90-85B engine was used to represent the most current in-use technology. A next-generation subsonic engine cycle, here called the Advanced

Table 3: NO Emissions Degradation Factors
[Adapted from Platt and Norster (1979), Table 45, p. 180]

Degradation Factor (% per 1000 hrs.)		EI at Climb		EPAP	
Engine Type	No. Units	Avg. Value	Deviation	Avg. Value	Deviation
JT8D-9	14	-3.3	±3.0	2.3	±2.6
JT8D-7	18	-3.8	±2.3	-3.2	±4.8
JT3D-7	9	-1.0	±1.9	-4.2	±3.6
JT3D-3B	13	-1.2	±3.1	-3.1	±2.6
JT9D-3A	9	-3.9	±3.6	-5.7	±4.5
RB211	10	5.3	±7.5	3.6	±5.9
CF700	9	-14.3	±12.7	-12.7	±18.3

Subsonic Engine (ASE), was established based on parameters from a cycle deck developed through a NASA-industry study (Liebeck *et al.*, 1995). The ASE cycle is representative of an engine for a medium range, 275 seat passenger aircraft with an entry-into-service of 2005. Finally, the supersonic cycle was based on engine parameters for a possible future European high-speed civil transport (EHSCT) with a Mach number of 2.0 as described by Habrard (1990). Table 4 gives an overview of the primary characteristics of these four cycles. Note that these cycles span a range of combustor inlet pressures (P_{T3} = 906-1371 kPa at cruise) and temperatures (T_{T3} = 732-954 K at cruise), and involve two types of engines; subsonic turbofans, including ultra-high bypass configurations, and a supersonic turbojet.

These cycles were developed using the commercially available cycle deck GASTURB (Kurzke, 1995). Cycles were specified as completely as possible, employing data available in the open literature for primary (*e.g.* bypass ratio, pressure ratios, total mass flow, and T_{T4}) and secondary (*e.g.* bleeds, cooling air, *etc.*) cycle parameters. Cycles were matched to performance data primarily through iterations on values for T_{T4}, and less so through alterations of component efficiencies, pressure ratios, and some secondary parameters. Several minor parameters were set to typical values. Cycle results were compared to typical published performance data for both design and off-design conditions resulting in the estimated differences in thrust and SFC shown in Table 5.

The differences between the results of the representative cycles and the published information are due primarily to the lack of data available for parameter specification, but it is worthwhile to consider some of the details of the cycle calculation. GASTURB references generalized component maps for the fan, compressors, and turbines for calculation of design and off-design operating points. When an efficiency or mass flow change was imposed on the cycle to simulate degradation, the map was scaled by the specified percentage. For example, when the efficiency of the high-pressure compressor was reduced by 1%, the contours on the generalized component maps were scaled by a factor of 0.99. For off-design analysis, the use of generalized component maps will cause some error and specific maps are always preferred. However, component maps for the engines studied are proprietary and were not available for this study. Though an operating line for the engines simulated can be generated, there was no data available with which to compare the results. In light of these considerations, we again emphasize the representative nature of the cycles developed for this study. The results presented in Section 4 do not necessarily reproduce the results one would find if the engines simulated were actually tested.

Table 4: Engine Cycle Parameters for the Cruise Condition

	CF6-50C2	GE90-85B	ASE	EHSCT
Altitude (m)	10668	10668	10688	18228
Mach No.	0.8	0.8	0.8	2.0
Thrust (kN)	47.6	76.9	27.9	40.4
SFC	19.0	16.7	14.5	32.4
Bypass Ratio	4.2	8.4	10.7	0.0
OPR	29.8	38.1	45.0	17.0
T_{T4} (K)	1440	1750	1610	1525
$W_{2,\,Corr.}$ (kg/s)	684	1325	686	190

Table 5: Comparisons of Developed Cycles and Published Data at Cruise and SLS Conditions

	CRUISE					
Engine	Cycle SFC	Pub. SFC	Est. SFC % Err.	Cycle Thrust	Pub. Thrust	Est. Thrust % Err.
CF6	19.0	17.7 [1]	-4.4	47.6	49.0	2.8
GE90	16.7	14.6 [2]	-14.0	76.9	77.9 [2]	1.2
ASE	14.5	14.6 [4]	0.7	27.9	30.3 [4]	7.8
EHSCT	32.4	32.2 [5]	-0.6	40.4	42.0 [5]	3.8
	SEA LEVEL STATIC					
CF6	11.0	10.8 [3]	2.6	236.5	230.4 [3]	1.7
GE90	8.9	8.1 [3]	9.9	393.5	395.3 [3]	0.5
ASE	NOT AVAILABLE					
EHSCT						

Sources:
[1] Mattingly, J.D. *(*1996).
[2] General Electric (1992).
[3] ICAO (1995).
[4] ASE cycle deck, NASA Lewis Research Center; see also Liebeck, R.H., *et al.* (1995).
[5] Harbrard, A. (1990).

3.2 Methods for Correlating Changes in Performance Parameters with Changes in NO_x Emissions Levels

In order to complete the task set out in this paper, the additional step of correlating engine operation with NO_x emissions levels is required. Correlations of NO_x emissions are of three basic types, all based on engine performance and emissions data obtained via combustor rig tests or full-scale engine tests at ground-level and/or at altitude. The first type, a *reference correlation,* uses sea level and altitude emissions data to formulate emissions correlations as ratios of engine conditions at altitude to those at sea level. A second, *direct correlation* formulation can be constructed using regression analysis of measurable test parameters (*e.g.* T_3, T_4, P_3) and/or consideration of time scales of chemical kinetics (*e.g.* t_{res}, P_{comb}, T_{adiab}). Such direct correlations typically employ data to formulate general dependencies on engine parameters and then these dependencies are tailored to specific combustor designs through multiplicative or additive constants that contain representations of the residence time, *etc.* The third type of correlation, a *fuel flow correlation,* was advanced in response to the inadequate availability of often proprietary engine test data and correlates corrected emissions results with corrected fuel flow and ambient conditions (see *e.g.* Boeing, 1995).

Most $EINO_x$ correlations exhibit a basic dependence on the combustor pressure raised to a power typically between 0.4 -0.6 and an exponential dependence on the temperature at the combustor inlet. Beginning with the Climatic Impact Assessment Program (CIAP, 1971-1975), $EINO_x$ dependencies of this type were used for several engine tests, including the engine variability and degradation tests discussed earlier in Section 2.4 (Prather *et al.*, 1992). Because of their usefulness in summarizing emissions characteristics, other public and private interests have continued to formulate correlations based on engine parameters that are sometimes made available in the open literature. However, these published correlations are usually for either older technology or for experimental combustion systems. In general, a standard correction for humidity is applied to the data used for all of these equations (see ICAO, 1993), although this correction is sometimes included explicitly in the EI correlation. In addition, because these equations usually refer to emissions exiting the combustor, they may not necessarily correspond directly to the emissions exiting the exhaust nozzle. However, Lukachko *et al.* (1996) have shown in a study of turbine and exhaust nozzle chemistry that for NO_x there is typically little change in emissions levels due to kinetics occurring within the engine downstream of the combustor.

Several correlations have been published in the open literature for specific aircraft engines and variants (*e.g.* Platt and Norster, 1979; Prather *et al.*, 1992; Lister *et al*. in Schumann *et al.*, 1995). A recent study on the usefulness of various correlations was presented by Lister *et al.* as part of the European AERONOX program (1995). This study considered the applicability of nine possible correlation equations of the three types described above for the prediction of NO_x from four different turbofan engine types. Lister *et al.* concluded that if the parameters used in $EINO_x$ equations of the direct correlation type were referenced to ground level certification data, the average variability in predictions for an engine at altitude was ±18%. Ground level and altitude tests of two engines showed that correlations specifically formulated for use with a particular engine are more accurate but emissions can be adequately estimated by the application of other correlation equations to those engines with preference given to use in a reference mode. Lister *et al*. suggest that in the development of global inventories, the use of any particular NO_x correlation equation will have an uncertainty (typically ±15-20%) smaller than other sources of inventory error, if referenced to certification data as described above. The accuracy of any correlation is limited by availability of data on which to construct the correlation. To achieve greater accuracy in the determination of engine data, emissions correlations specific to the engine considered are required. Lister *et al.* did not consider the effect of changing technology, such as correlations appropriate for dual-stage combustors.

3.3 Application of $EINO_x$ Correlations

The emissions correlations used with the cycles in this study are given in Table 6. They are of the direct correlation type and most are of a mixed character, employing both characteristic time and parameter regression in their construction as discussed in Section 3.2. The correlation used for the EHSCT is based solely on a characteristic time formulation.

In applying these correlations, it was assumed that all effects of aging are realized as changes in T_3, P_3, T_4, the combustor residence time (t_{res}), and the adiabatic flame temperature (T_{adiab}), rather than through changes in the empirical constants used in the correlations. *It is believed that this assumption is the primary source of uncertainties for the conclusions presented in this paper*. More information about the correlations and the derivation of the empirical constants would be necessary to properly validate the accuracy of this assumption.

Table 6: $EINO_x$ Correlations Used with Simulated Engine Cycles

Engine	NO_x Correlation as $EINO_2(NO_x)$
CF6-50C2 [1]	$1.35 \cdot 0.0986 \cdot \left(\frac{P_3}{1\ atm}\right)^{0.4} \exp\left(\frac{T_3}{194.4\ K} - \frac{H_0}{53.2\ g\ H_2O/kg\ dry\ air}\right) + 1.7$
GE90-85B[2]	$0.0986 \cdot \left(\frac{P_3}{1\ atm}\right)^{0.4} \exp\left(\frac{T_3}{194.4\ K} - \frac{H_0}{53.2\ g\ H_2O/kg\ dry\ air}\right)$
ASE[3]	$0.0041941 \cdot T_4 \cdot \left(\frac{P_3}{439\ psia}\right)^{0.37} \exp\left(\frac{T_3 - 1471\ R}{345\ R}\right)$
EHSCT [4]	$t_{res} \cdot \exp\left(-72.28 + 2.8\ T_{adiabatic}^{0.5} \frac{T_{adiabatic}}{38.02}\right)$

Sources:
[1] [2] Gleason and Bahr (1979).
[3] Bill Haller, NASA Lewis, personal communication.
[4] Roffe and Venkataramani (1978).

Table 7: Comparison of Calculated $EINO_x$ Using Simulated Cycles with Emissions Certification Data

Engine	Simulated $EINO_x$ at cruise	Simulated Engine Combustor	ICAO $EINO_x$ PL = 30%	ICAO $EINO_x$ PL = 85%	Certification Engine Designation	Certification Engine Combustor
CF6-50C2	16.5	single annular	9.50	29.70	CF6-50C1 or -50C2	single annular
GE90-85B	13.8	double annular	10.30	40.27	GE90-85B	double annular
ASE	8.9	double annular	—	—	—	—
EHSCT	6.1	LPP	3.5	9.3	Olympus 593 Mk 610	single annular

Note: Olympus power settings are actually 34% for the value in 30% power level (PL) column and 65% in 85% column.

The correlation used for the CF6-50C is applicable directly to the cycle simulations introduced in this paper. Drawing from the work of Lister *et al.*, the accuracy of the correlation should be better than the ±15-20% result obtained for the application of a nonspecific correlation. For the GE90-85B, no emissions correlation is publicly available, but it is known that the GE90-85B employs a dual-annular, staged combustor design that owes some of its design to concepts developed through the NASA Experimental Clean Combustor Program (ECCP). The ECCP, in association with General Electric, produced emissions correlations for the CF6-50C (*e.g.* the equation shown in Table 6), the CF6-80C, and an advanced, dual-annular, low-NO_x combustor concept. This dual-annular emissions correlation is thought to capture the basic emissions characteristics of the GE90 engine. The coefficients used for the CF6-50C and dual-annular correlations include parameters describing specific combustor design details such as residence time. While for the CF6-50C2 these parameters will remain essentially the same, no attempt was made to change these parameters for the dual-annular case to match the GE90-85B combustion system.

The ASE engine employs a dual-annular, staged combustor and since the ASE is a concept engine cycle, the correlation employed is based on projected behavior. An ultra-low-NO_x correlation based on tests of the lean-premixed prevaporized (LPP) concept was employed as representative of HSCT emissions characteristics (Roffe and Venkataramani, 1978). This equation predicts emissions based on t_{res} and T_{adiab}. For this paper, the adiabatic flame temperature was assumed to be 2000 K and the residence time was calculated using a simplified model of a constant area, viscous duct with constant pressure and prescribed temperature change. Using cruise condition engine parameters for the simulated cycles, $EINO_x$ results were compared with certification emissions data given in the ICAO Engine Exhaust Emissions Data Bank (1995) in Table 7. For the LPP combustor case, certification data for the Concorde Olympus engine is provided for reference. The low-NO_x emissions goal of the NASA High-Speed Research Program is for an $EINO_x$ of 5 g/kg fuel.

4. RESULTS

Changes in pollutant emissions with time are a strong function of the pattern of degradation for a particular engine, the components that are degraded, the magnitude and combination of efficiency and flow capacity change, and the technology represented by the engine design, both the cycle and the type of combustor utilized. The GASTURB cycle deck was used to perform aging investigations through changes in component efficiencies and flow capacities. Both sensitivity and scenario analyses are presented in the following sections, including a description of the calculation methodology and specifics about the GASTURB implementation. The analyses reveal both broad technological and specific component trends and provide an overview of the aging effect that proves useful for understanding the impact of deterioration on emissions levels. In order to place the results in context, the limit to deterioration suggested previously, a 3% increase in SFC, is applied to the results to bound the changes observed in the NO_x emissions rate.

4.1 NO_x Emissions Sensitivity to Small Component Perturbations

Influence coefficients comparing the emissions and thermodynamic performance of new and degraded engines were generated using one percent perturbations to individual component efficiencies and flow capacities. Where component efficiency will typically decrease with age for both the compressor and turbine, flow capacity changes with age typically differ for a compressor and turbine. For a compressor, flow capacity is likely to decrease, primarily due to fouling and increased aerodynamic blockage due to blade tip clearance increases and other effects. Conversely, for the turbine, erosion and other thermal damage increase the size of blade passages and thus the flow capacity. The perturbed state was calculated via a design calculation under the constraint of constant thrust at the cruise condition. This constraint is based on typical flight procedures where a given Mach number, usually between 0.8 and 0.85 at cruise, is set for the duration of the flight. Using GASTURB, the constraint of constant thrust can be set directly through iterations on component matching.[1]

[1] In practice, an indicator is used to set the thrust. Typically, this is the low-pressure spool speed, N1, or the engine pressure ratio, EPR. Considering the alternative practice, the constraint of constant N1 was also examined. Results show similar orders of magnitudes and signs for sensitivities but the actual values vary on the order of 10 - 15%.

Table 8: Parameter Sensitivity Results for Subsonic, Turbofan Cycles at Cruise Condition

BASELINE VALUES	CF6-50C2					GE90-85B				
	T_{T3} (K)	P_{T3} (atm)	T_{T4} (K)	SFC (g/kN s)	NO_x/s (g/s)	T_{T3} (K)	P_{T3} (atm)	T_{T4} (K)	SFC (g/kN s)	NO_x/s (g/s)
	732	10.7	1440	19.0	15.0	758	13.5	1750	16.7	17.7
PARAMETER	T_{T3} (K)	P_{T3} (%)	T_{T4} (K)	SFC (%)	NO_x/s (%)	T_{T3} (K)	P_{T3} (%)	T_{T4} (K)	SFC (%)	NO_x/s (%)
-1% eff. fan	0.00	0.16	1.05	0.29	0.35	0.66	0.21	3.31	0.42	0.85
-1% eff. LPC	1.76	-0.01	3.59	0.19	1.00	1.68	-0.02	3.74	0.13	0.99
-1% eff. HPC	1.97	-0.33	7.00	0.26	1.06	2.58	-0.29	9.14	0.23	1.45
-1% HPC cap	0.32	-0.05	1.13	0.04	0.17	1.91	-0.21	6.75	0.17	1.07
-1% eff. HPT	-3.89	-0.63	3.18	0.29	-1.71	-4.49	-0.57	4.87	0.26	-2.25
+1% HPT cap	-2.51	-1.13	-0.02	0.12	-1.44	-2.95	-1.14	0.32	0.08	-1.87
-1% eff. LPT	0.34	0.27	2.83	0.57	0.82	1.34	0.30	5.96	0.67	1.49
+1% LPT cap	2.33	0.41	1.32	0.26	1.49	2.79	0.42	0.85	0.23	1.85

BASELINE VALUES	ASE					EHSCT				
	T_{T3} (K)	P_{T3} (atm)	T_{T4} (K)	SFC (g/kN s)	NO_x/s (g/s)	T_{T3} (K)	P_{T3} (atm)	T_{T4} (K)	SFC (g/kN s)	NO_x/s (g/s)
	801	16.0	1611	14.5	3.6	954	8.9	1525	32.4	8.0
PARAMETER	T_{T3} (K)	P_{T3} (%)	T_{T4} (K)	SFC (%)	NO_x/s (%)	T_{T3} (K)	P_{T3} (%)	T_{T4} (K)	SFC (%)	NO_x/s (%)
-1% eff. fan	0.47	0.28	2.32	0.48	0.97	—	—	—	—	—
-1% eff. LPC	1.78	-0.02	3.55	0.14	1.29	—	—	—	—	—
-1% eff. HPC	2.30	-0.35	7.74	0.21	1.77	2.90	-0.37	7.56	0.36	0.40
-1% HPC cap	0.39	-0.06	1.30	0.04	0.30	0.76	0.04	0.92	0.02	0.01
-1% eff. HPT	-4.44	-0.69	3.47	0.23	-2.10	-4.95	-0.77	2.36	0.47	0.82
+1% HPT cap	-2.59	-1.13	-0.15	0.08	-1.68	-2.88	-1.09	-0.80	0.12	0.10
-1% eff. LPT	0.91	0.41	4.09	0.74	1.63	—	—	—	—	—
+1% LPT cap	2.41	0.41	0.87	0.21	1.69	—	—	—	—	—

Table 8 shows cycle parameter changes resulting from small perturbations (1% change with sign depending on parameter) to component efficiencies and flow capacities for each of the cycles simulated. Included in the table is the relative change in NO_x/s, which is the product of the $EINO_x$ and the fuel flow rate.

The results in Table 8 indicate that changes in the HPT and HPC component efficiencies and in the HPT flow capacity produce the largest changes in cycle parameters and also the largest changes in NO_x/s. If we compare these results to the limits on component degradation suggested in Table 1, we see that changes in NO_x/s of up to ±12% may be possible. However, as is shown in Section 4.3, typical changes in NO_x/s are expected to be much smaller than this, due in large part to the competing influences of HPC and HPT degradation. For example, the influence coefficients show that for the HPT both flow capacity increases and efficiency decreases (the typical aging trends) lead to a decrease in the NO_x/s. However, for the HPC, the typical aging effects (decreases in both flow capacity and efficiency) lead to an increase in NO_x/s. Note that in all cases, faults increase the fuel flow rate. Thus, in terms of the total NO_x emitted (*e.g.* NO_x/s), an increase in $EINO_x$ is always exacerbated by the change in fuel flow and a decrease in $EINO_x$ is always attenuated. This is particularly noticeable for the EHSCT. Using the simple duct model to estimate residence time for the EHSCT $EINO_x$ equation, flow capacity changes reduce residence time while efficiency changes increase residence time, affecting a negative change in the $EINO_x$ for the former and a positive change for the latter. However, both the NO_x/s changes are both positive because the increased fuel usage overwhelms the slight decreases in the $EINO_x$.

The opposing influences of turbine and compressor faults can be illustrated using temperature-entropy (T-s) diagrams for the Brayton cycle as shown in Figure 2. If the cycle is constrained to result in the *same work*, losses in compressor efficiency tend to cause increases in both T_3 and T_4 as shown in Figure 2a. However, for constant work, losses in turbine efficiency tend to depress T_3 and produce relatively smaller increases in T_4 as shown in Figure 2b.

Similar arguments can be made for the relative effects of each of the component faults modeled, however the arguments are more complicated because of the complexity of the two-spool turbofan

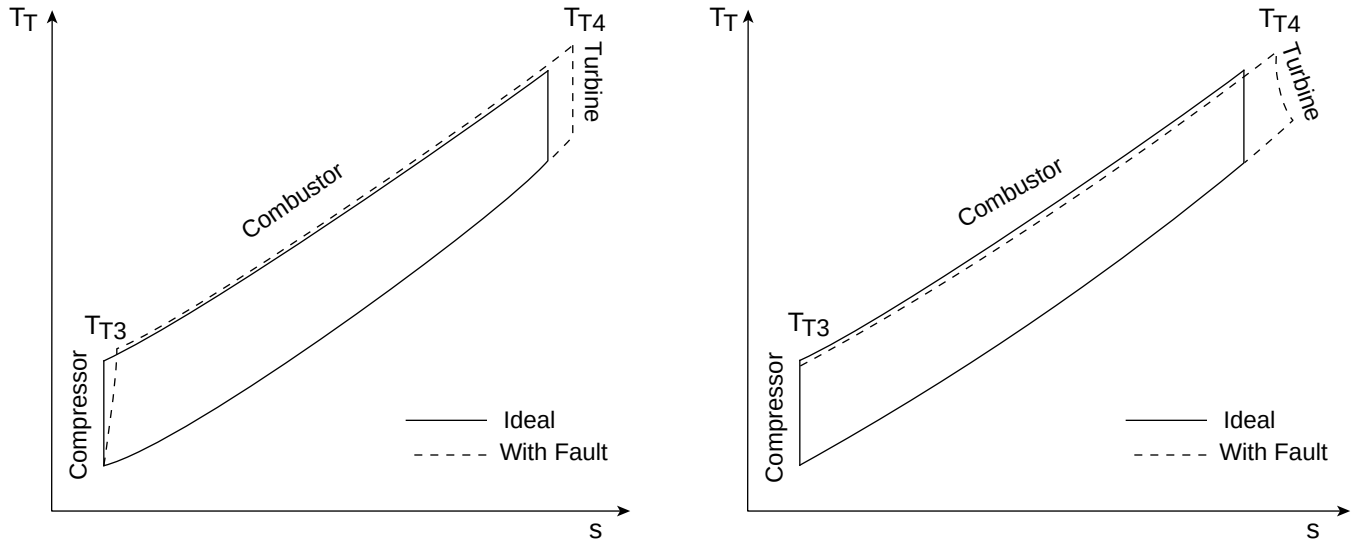

a) Effect of compressor deterioration at constant work.

b) Effect of turbine deterioration at constant work.

Figure 2: The opposing influences of turbine and compressor faults on engine parameters; temperature-entropy diagrams for single-spool turbojet cycles.

cycles investigated. We give only one example below for the different effects of HPT and LPT capacity changes.

Sensitivity results indicate that for turbofans, an increase in HPT capacity leads to a decrease in NO_x/s whereas an increase in LPT capacity leads to an increase in NO_x/s. These opposing influences can be explained by considering that the LPT is responsible for powering the fan where 70-90% of the thrust can be generated. Both of these component faults lead to larger mass flows and, at the same efficiency, less work per kilogram. Increased flow capacity leads to a lower compressor discharge pressure (P_{T3}) and temperature (T_{T3}) which prompt an increase in fuel flow until the original thrust level is achieved. The additional mass flow also leads to an increase in thrust which offsets some of the thrust decrease due to lower pressure ratios. However, for the LPT capacity increase, the fan is also affected and a larger thrust decrease is realized because of the LPT fault than for the HPT fault. The result is that for the HPT capacity increase, there is a net decrease in P_{T3}, T_{T3}, and T_{T4} (in all cases except of the GE90-85B) whereas for the LPT fault, there is an increase in all these parameters. The decreases in the HPT case lead to decreases in $EINO_x$, which, depending on the magnitude of the increased fuel requirement, is manifest as a smaller percent decrease in NO_x/s. For the LPT, all trends favor an $EINO_x$ increase with age which is exacerbated by the increased fuel needs, leading to an even higher percent change in NO_x/s.

4.2 Technological Trends

As gas turbine technology has advanced, engine pressure ratios and cycle temperatures have increased to achieve better fuel efficiency. Correlating the results shown in Table 8 with the cycle OPR and T_{T4} illustrates the changes in sensitivity of NO_x emissions to aging effects that occur as technology advances. As shown in Figure 3, changes in NO_x/s increase with increasing OPR for the fan, HPC, LPC, and LPT efficiency faults. Increased sensitivity of NO_x/s with increased T_{T4} is shown in Figure 4 for HPC, HPT, and LPT capacity faults and HPT efficiency faults.[2] Thus, NO_x emissions from more technologically advanced cycles are more sensitive to aging.

4.3 NO_x Emissions Results for Sample Degradation Scenarios

Sample degradation scenarios were imposed on each of the four cycles using degradation of the high-pressure turbine (HPT) and the high-pressure compressor (HPC) both separately and in combination. The HPT and HPC were chosen for further calculations because anecdotal information from engine manufacturers suggests that degradation of these components is the largest contributor to overall engine aging trends. Table 9 summarizes the scenarios investigated. One point of efficiency loss was combined with one point of flow capacity change, the latter being positive for the HPT and negative for the HPC. For the combined HPT and HPC aging scenario, it was assumed that the degradation of

[2] Figures 3 and 4 indicate that the EHSCT cycle exhibits much less sensitivity to efficiency and flow capacity changes at cruise than any of the turbofan cycles. However, most HSCT engine concepts are of the variable cycle type (Harbard, 1990; Boeing, 1989) and it is unclear whether the aging behavior of a multiple cycle engine will exhibit a similar degradation sensitivity to the single spool turbojet cycle.

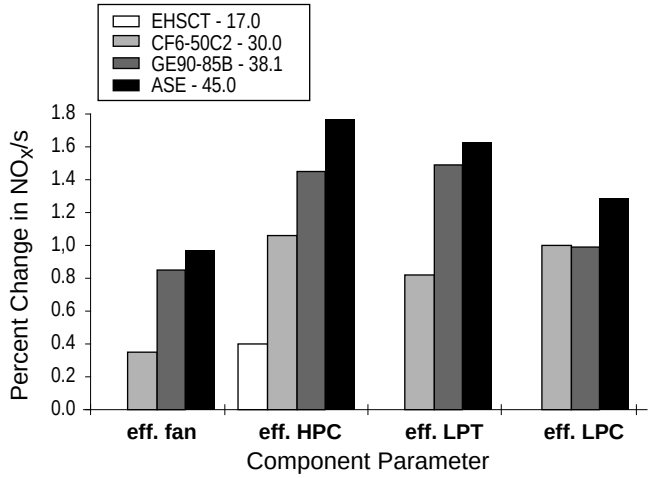

Figure 3: Change in NO_x/s resulting from component parameter degradation: trends with OPR.

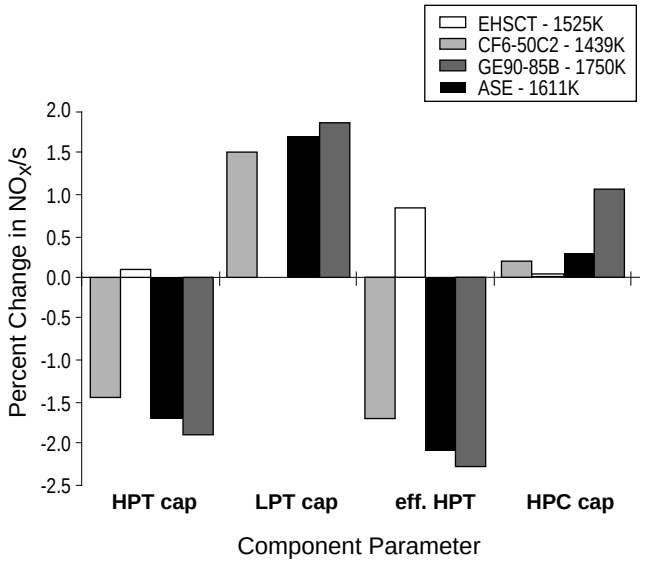

Figure 4: Change in NO_x/s resulting from component parameter degradation: trends with T_{T4}.

the turbine and compressor occur with the same efficiency loss and capacity change per unit time. This choice was again based on anecdotal evidence for current engines which suggests that, while individual engines have unique aging profiles, on average for a group of engines, compressors and turbines will degrade at approximately the same rate. Scenario calculations were conducted through off-design matching, using the constraint of constant thrust at the cruise condition.

The results previously presented in Table 8 show that HPT degradation leads to *decreases* in NO_x/s while compressor and LPT faults lead to *increases* in NO_x/s. These trends are borne out in the results of the aging scenarios shown in Figures 5 and 6 for HPT-only and HPC-only faults respectively. To relate these results to maintenance practices, the NO_x changes (solid lines) are plotted with the corresponding changes in SFC (dashed lines), marking the overhaul condition by the +2-4% SFC threshold. The relative linearity of these trends suggests that influence coefficients presented in Table 8 are useful for predicting changes in emissions mass flow even for large changes in component performance.

Table 9: Assumed Degradation Scenarios

	HPT-Only		HPC-Only		HPT and HPC Combined			
Level	% HPT eff.	% HPT cap.	% HPC eff.	% HPC cap.	% HPT eff.	% HPT cap.	% HPC eff.	% HPC cap.
0	0.00	0.00	0.00	0.00	0.00	0.00	0.00	0.00
1	-1.00	1.00	-1.00	-1.00	-1.00	1.00	-1.00	-1.00
2	-2.00	2.00	-2.00	-2.00	-2.00	2.00	-2.00	-2.00
3	-3.00	3.00	-3.00	-3.00	-3.00	3.00	-3.00	-3.00
4	-4.00	4.00	-4.00	-4.00	-4.00	4.00	-4.00	-4.00
5	-5.00	5.00	-5.00	-5.00	-5.00	5.00	-5.00	-5.00
7	-7.00	7.00	-7.00	-7.00	---	---	---	---
9	-9.00	9.00	-9.00	-9.00	---	---	---	---

For the HPT-only scenario, increased degradation levels result in lower compressor discharge pressure and temperature and a higher T_{T4}, which lead to a higher fuel flow and, at constant thrust, a higher SFC. The effect on the $EINO_x$ is negative, that is *lower* emissions per fuel burned for higher degradation levels, for all cases other than the EHSCT cycle. The $EINO_x$ decrease is tempered somewhat by the increase in fuel flow necessary to power the now progressively less efficient engine. For the HPC-only degradation case, a lower P_{T3} and higher T_{T4} result as with the HPT-only case, but the combustor inlet temperature increases. The efficiency effects are again similar, since the HPC-only aging leads to a higher fuel flow and thus higher SFC at constant thrust. The effect on the $EINO_x$ is positive, meaning higher emissions per unit fuel flow. Since the fuel flow also increases, it enhances the effect leading to even higher changes in the value of NO_x/s.

For the HPC-only scenario, using a limit of a 3% SFC rise before overhaul would result in a degradation level of between 5 and 7 for turbofan cycles and a degradation level of about four for the EHSCT case. These correspond to 10-25% and 1% increases in NO_x/s, respectively. SFC for newer cycles is less sensitive to aging and thus the cycles tend towards higher degradation levels before exceeding the overhaul limits. For the HPT-only scenario, the SFC criteria is exceeded at a degradation level of between 4 and 6 for turbofan cycles and at level two for the EHSCT. These correspond to a -8% to -14% and +1% changes in NO_x/s respectively. Where the HPC-only cases show marked differences in degradation effect as a function of the turbofan cycle simulated, and higher increases in the percent change in NO_x/s with degradation level, the HPT-only cases show remarkably simi-

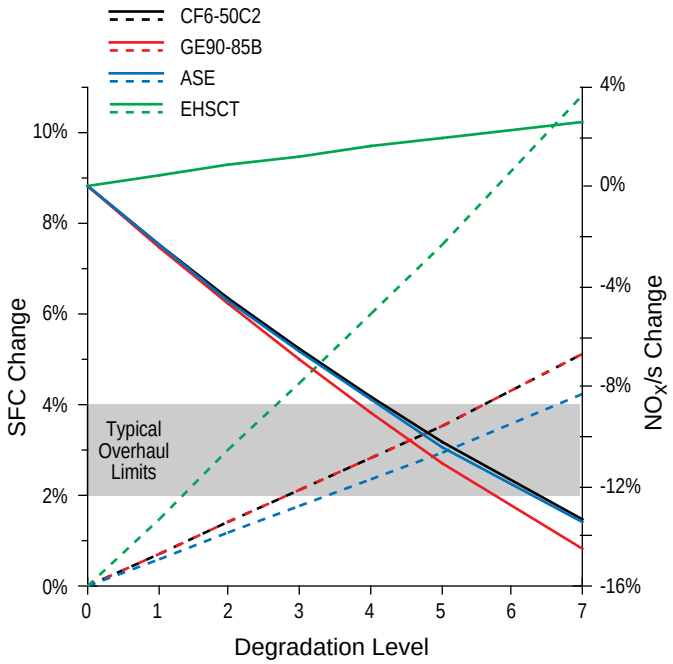

Figure 5: Percent changes in NO_x/s (solid lines) as a function of degradation level: HPT-only scenario. (SFC changes are shown with dashed lines.)

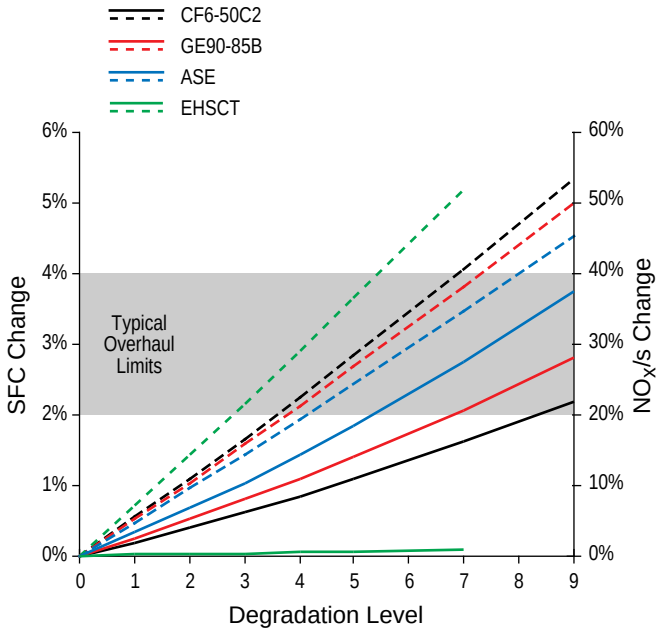

Figure 6: Percent changes in NO_x/s (solid lines) as a function of degradation level: HPC-only scenario. (SFC changes are shown with dashed lines.)

lar patterns of emissions change across all turbofan cycles. The EHSCT case, exhibiting increases in NO_x for both HPT and HPC degradation, shows a lower sensitivity to degradation. However, as with all the cycles, these numbers must be viewed in the context of the original values of NO_x/s for the cruise condition without aging (see Table 8).

While the HPT-only and HPC-only scenarios illustrate the opposing influences of turbine and compressor aging, the combined HPT and HPC aging scenario is expected to be more representative of typical engine aging behavior. Combined degradation of the HPC and HPT results in an almost linear change in cycle parameters exemplified by Figure 7 for the CF6-50C2 cycle. All cycles modeled exhibit similar trends and magnitudes of change in T_{T3}, P_{T3}, and T_{T4} to those shown for the CF6-50C2. However, the way in which these changes effect the $EINO_x$ and subsequently the NO_x/s value is not similar for the different cycles. It was noted earlier that fuel flow always increases with degradation, enhancing an increase in $EINO_x$ and attenuating a decrease. This differential effect among the cycles is noted in Figure 8 where the CF6-50C2 cycle experiences a decline in NO_x/s with increasing degradation level as a percentage of the baseline while all other cycles show increases. The largest changes are seen for the ASE cycle. For all of the cycles, the $EINO_x$ value actually decreases, except for the ASE where the value fluctuates near zero. Thus, the effect of fuel flow increases due to the less efficient cycles is enough to increase the emissions flux and negate the gains in the $EINO_x$. The +3% SFC criteria is exceeded at a degradation level of between 2 and 3 for turbofan cycles and above level 1 for the EHSCT. These correspond to -1% to +4% and +3% changes in NO_x/s, respectively.

These results compare well with the only published empirical data (Platt and Norster, 1979) regarding the effects of engine aging on aircraft emissions. Examination of the Platt and Norster results, which are summarized in Table 3, shows there was a relatively small effect on NO_x emissions from deterioration. The measured changes in emission rates were on the order of the unit to unit deviation. The Platt and Norster results, however, do generally indicate a decrease in EINO.[3] Further investigation of the maintenance records supplied with the report shows at least one engine's history exhibits a majority of HPT problems (the JT3D). This observation is in general agreement with the results for the HPT noted in the current study. For the CF6-50C2 cycle studied here, a reduction of 11% in the $EINO_x$ value is realized with the SFC limitation for the HPT-only scenario and a -3.5% $EINO_x$ change for the combined case. At overhaul time for the JT3D, the rate reported by Platt and Norster would give a decrease of -2.8 to -3.6% in $EINO_x$ for 2300-3000 hours of operation.

[3] EINO is comparable to $EINO_x$ since ~90% of the NO_x emitted is emitted as NO.

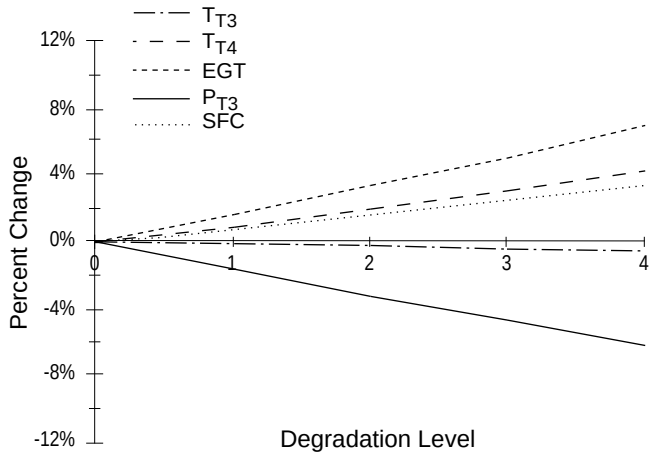

Figure 7: Changes in operational parameters: CF6-50C2, HPT + HPC degradation scenario.

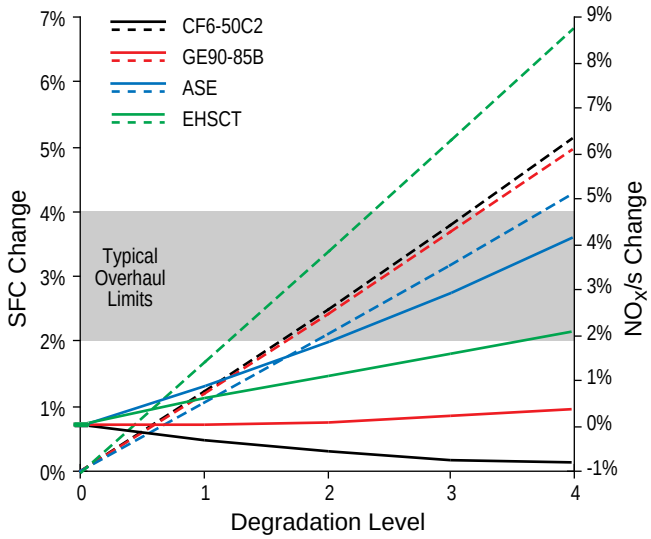

Figure 8: Percent changes in NO_x/s (solid lines) as a function of degradation level: HPT + HPC scenario. (SFC changes are shown with dashed lines.)

5. IMPACT ON EMISSIONS INVENTORIES

The results of the previous section provide a wide scope with which to view the effect of aging on engine NO_x emissions. It is possible to draw some conclusions regarding emissions inventories used by assessment programs to initialize atmospheric NO_x distributions and magnitudes in global modeling studies. There are currently two emissions inventories under development, one a joint effort between Boeing and McDonnell-Douglas for the NASA Atmospheric Effects of Aviation Project and the other a European effort supported by the European Civil Aviation Conference (ECAC) through its Abatement of Nuisances Caused by Air Transport (ANCAT) group which is responsible for environmental issues. Each of these projects attempts to predict fleetwide emissions loadings over altitude, latitude, and longitude through models of flight profiles, emission indices, and aircraft/engine performance for both commercial and non-commercial schedules. Where the ECAC/ANCAT inventory employs a common, ratio type NO_x correlation among all aircraft, the NASA inventory uses the Boeing fuel flow methodology (see Section 3.2). There are many uncertainties related to the use of these inventories. Inaccurate or incomplete movement data, erroneous flight profiles, aircraft performance data, or aircraft condition with respect to weight or fuel loading, assumptions regarding routing, $EINO_x$, and the contributions of classified military flights can all have an effect on the final results. It is known that these inventories do not account directly for the effects of aging on emissions. The key question is whether the effects of aging are significant compared to the current uncertainties in these inventories.

Fuel burn for the NASA inventory is calculated to be on the order of 10 - 20% lower than US Department of Transportation reported fuel use data for a US airlines based validation test (Stolarski and Wesoky, 1993). For the entire global inventory, a 76% match in fuel-use was realized as compared to International Energy Agency data, for an overall NO_x burden of 1.92 Tg/yr corresponding to an average $EINO_x$ of 10.9 for the base year 1990. The ECAC/ANCAT effort indicates that deviations from great circle routing could result in an approximately 10% increase in fuel burn (Schumann *et al.*, 1995). In addition, ECAC/ANCAT also notes that lack of performance data for engines will have a subsequent effect on the NO_x emissions level because the methodology used requires simulations of aircraft performance and derivation of NO_x emissions much like the current study. Conducting a validation test comparing a simulated flight with actual performance data and using the generic $EINO_x$ correlation, they estimate that variability in fuel burn and emissions production could be ±10% due to inaccuracy in performance simulations. The results here add another level of complexity to these considerations in the form of aging. If we determine from these brief comments that uncertainty in the inventories is at least 10% and perhaps greater than 25%, the results given for HPT-only, HPC-only, and the combined scenario NO_x/s changes of -8 to -14%, +10 to +25%, and -1 to +4%, respectively, would seem to be on the order of or less than the uncertainties currently found in the inventories. In addition, if we rely more on the combined scenario to represent the probable path of degradation, it is more likely that aging effects would currently be small compared to other inventory uncertainties.

6. SUMMARY AND FURTHER RESEARCH

This paper has presented research concerning the effect of engine aging on NO_x emissions for a range of aircraft engines representing different technologies. The results indicated that for subsonic turbofans, HPC, LPC, fan and LPT faults increase NO_x

emissions flux whereas deterioration of the HPT decreases NO_x emissions flux. Aging of the HPT and HPC have the largest effect on cycle parameters and NO_x emissions. Increased sensitivity of NO_x/s with increasing OPR or T_{T4} was also observed. For the supersonic case, all degradation scenarios led to increased emissions, however, the sensitivity to changes in cycle parameters was smaller than for the subsonic cases. In all cases, both turbine and compressor faults, an increase in $EINO_x$ is exacerbated by the change in fuel flow and a decrease in $EINO_x$ is attenuated.

Scenario calculations confirmed the usefulness of the influence coefficients indicating fairly linear changes in cycle parameters with increasing degradation level for the HPT-only, HPC-only, and HPT + HPC aging cases. For a 3% SFC rise overhaul limit, decreases in NO_x/s for turbofans with HPT-only aging for all simulations fell between -8% and -14% and increases in NO_x/s for HPC deterioration were between +10% and +25%. Combining these aging effects resulted in a -1% to +4% change in the emissions flux. For the supersonic case, changes were much smaller, with a 3% SFC limitation resulting in +1% changes for both HPT-only and HPC-only scenarios, and +3% for the combined case.

There are several sources of uncertainty in these analyses of aging effects. Primarily, these uncertainties are associated with the lack of performance data and empirical information on the effects of aging on engine emissions and with the lack of detailed information regarding the NO_x correlations used. Increased availability of these elements could be used to build more widely relevant representative engine cycles and to provide a better database through which to validate the results presented.

Application of these results to the improvement of emissions inventories used for analysis of the atmospheric effects of aviation would seem to be premature due to the greater uncertainties in other inventory elements. However, regardless of the current applicability of these results to emissions inventories, attention to the effects of engine aging on aircraft NO_x emissions would seem to be warranted in anticipation of broader consideration of these issues that could come about due to rapid improvements of the inventories or perhaps more indirectly through regulatory action.

7. ACKNOWLEDGMENTS

We thank Chowen Wey and Bill Haller of the NASA Lewis Research Center for providing information on the ASE engine cycle. We also appreciate the insight and advice regarding engine aging provided by Alan Epstein of the MIT Gas Turbine Laboratory. Finally, we thank Diana Park for help with editing and production of this paper.

8. REFERENCES

43 FR 58, EPA, "Control of Air Pollution From Aircraft and Aircraft Engines: Proposed Amendments to Standards," *Federal Register*, pp. 12615-12634, 1978.

47 FR 251, EPA, "Emissions Standards and Test Procedures," *Federal Register*, pp. 58461-58474, 1982.

55 FR 155, DOT, "Fuel Venting and Exhaust Emission Requirements for Turbine Engine Powered Airplanes; Final Rule," *Federal Register*, pp. 32856-32866, 1990.

Aker, G.F. and H.I.H. Saravanamuttoo, "Predicting Gas Turbine Performance Degradation Due to Compressor Fouling Using Computer Simulation Techniques," *Transactions of the ASME: Journal of Engineering for Gas Turbines and Power*, Vol. 111, pp. 343-350, 1989.

Arnold, B.R. and J.R. Gast, "A Cooperative Airline Program to Evaluate Engine Parts Aging Effects on a Current Turbofan Engine Model," SAE Paper 700329, pp. 1032-1041, 1970.

Becker, E.E., G. Frings, and W.C. Cavage, "Exhaust Emissions Characteristics and Variability for Pratt and Whitney JT8D-7A Gas Turbine Engines Subjected to Major Overhaul and Repair: Final Report," FAA-CT-79-53, 1980.

The Boeing Company, Martin, R.L., "Appendix D. Boeing Method 2 Fuel Flow Methodology Description," presented to the CAEP Working Group III Certification Subgroup, 1995.

Dupis, R.J., H.I.H. Saravanamuttoo, and D.M. Rudnitski, "Modelling of Component Faults in Application to On-Condition Health Monitoring," ASME 86-GT-153, presented at the International Gas Turbine Conference and Exhibit, Dusseldorf, W. Germany, 1986.

Frings, G., "Exhaust Emission Characteristics and Variability for Maintained General Electric CF6-50 Turbofan Engines," FAA Report No. FAA-CT-80-36, Final Report, 1980.

Frith, P.C., "Diagnosis of Compressor Degradation in Helicopter Engines," 5th Australian Aeronautical Conference, Melbourne, Australia, 1993.

General Electric, *GE: The Leading Edge*, manufacturer's literature, 1992.

Gleason, C.C., and Bahr, D.W., "NASA Experimental Clean Combustor Program (ECCP)," NASA CR-135-384, 1979.

Harbrard, A., "The Variable-Cycle Engine to Meet the Economic and Environmental Challenge of the Future Supersonic Transport Aircraft," *Revue Scientifique SNECMA*, No. 1, 1990.

ICAO, International Civil Aviation Organization, *ICAO Engine Exhaust Emissions Data Bank*, ICAO Doc 9646-AN/943, 1st ed., 1995.

ICAO, International Civil Aviation Organization, *International Standards and Recommended Practices: Environmental Protection, Annex 16 to the Convention on International Civil Aviation, Volume II: Aircraft Emissions*, 2nd ed., 1993.

Kurzke, J., "GASTURB Version 6.0: A Program to Calculate Design and Off-Design Performance of Gas Turbines," 1995.

Lakshminarasimha, A.N., and H.I.H. Saravanamuttoo, "Prediction of Fouled Compressor Performance Using Stage Stacking Techniques," *ASME Symposium on Turbomachinery Performance Deterioration*, FED-Vol. 37, 1986.

Liebeck, R.H. *et al.*, "Advanced Subsonic Design and Economic Studies," *NASA CR-195443*, 1995.

Lukachko, S.P., I.A. Waitz, R.C. Miake-Lye, R.C. Brown, and M.R. Anderson, "Chemical Processes in the Turbine and

Exhaust Nozzle," presented at Comite Avion Ozone Impact of Aircraft upon the Atmosphere International Colloquium, Paris, 1996.

Lyon, T.F. and D.W. Bahr, "CF6-50 Engine Emissions Testing with Traverse Probe," FAA Report No. FAA-CT-81-18, conducted by General Electric Company, Aircraft Engine Business Group, Final Report, 1981.

Lyon, T.F., W.J. Dodds, and D.W. Bahr, "Determination of Pollutant Emissions Characteristics of General Electric CF6-6 and CF6-50 Model Engines, Final Report," FAA-EE-80-27, 1980.

MacIssac, B.D., "Engine Performance and Heaxth Monitoring Models using Steady State and Transient Prediction Methods." in *Steady and Transient Performance Prediction of Gas Turbine Engines*, NATO, AGARD-LS-183, 1992.

Mattingly, J.D., *Elements of Gas Turbine Propulsion*, McGraw-Hill, 1996.

NASA/ICAO, *NASA/ICAO Database — Research on Atmospheric Effects of Aviation*, maintained by H. Wesoky, 1996.

Platt, M. and E.R. Norster, "Time Degradation Factors for Turbine Engine Exhaust Emissions: Volume 1, Program Description and Results, Interim Report," FAA-RD-78-56 or N79-17860, 1978.

Platt, M. and E.R. Norster, "Time Degradation Factors for Turbine Engine Exhaust Emissions: Volume 1, Program Description and Results, Final Report," FAA-RD-79-8, 1979.

Prather, M.J. *et al*., *The Atmospheric Effects of Stratospheric Aircraft: A First Program Report*, NASA Reference Publication 1272, NASA Office of Space Science and Applications, Washington, DC, 1992.

Richardson, J.H., G.P. Sallee, and F.K Smakula, "Causes of High Pressure Compressor Deterioration in Service," AIAA/SAE,ASME 15th Joint Propulsion Conference, AIAA 79-1234, Las Vegas, Nevada, 1979.

Roffe, G., and K.S. Venkataramani, "Emission Measurements for a Lean Premixed Propane/Air System at Pressures up to 30 Atmospheres", NASA CR-159421, 1978.

Saravanamuttoo, H.I.H., and A.N. Lakshminarasimha, "A Preliminary Assessment of Compressor Fouling," ASME 85-GT-153, Gas Turbine Conference and Exhibit, Houston, Texas, 1985.

Saravanamuttoo, H.I.H., and B.D. MacIsaac, "Thermodynamic Models for Pipeline Gas Turbine Diagnostics," *Transactions of the ASME: Journal of Engineering for Power*, Vol. 105, pp. 875-884, 1983.

Schumann, U., ed., *AERONOX: The Impact of NOx Emissions from Aircraft Upon the Atmosphere at Flight Altitudes 8-15 km: Final Report to the Commission of European Communities*, Brussels, Belgium, EC-DLR, 1995.

Singh, D., A. Hamed, and W. Tabakoff, "Simulation of Performance Deterioration in Eroded Compressors," ASME 96-GT-422, 1996.

Stevenson, J.D. and H.I.H. Saravanamuttoo, "Effect of Cycle Choice and Deterioration on Thrust Indicators for Civil Engines," ISABE 95-7077, in *Twelfth International Symposium on Air Breathing Engines*, ed. F.S. Billig, Vol. 2, Melbourne, Australia, 1995.

Stolarski, R.S., and H.L. Wesoky (eds.), *The Atmospheric Effects of Stratospheric Aircraft: A Third Program Report*, NASA Reference Publication 1313, NASA Office of Space Science and Applications, Washington, DC, 1993.

Treager, I.E., *Aircraft Gas Turbine Engine Technology*, 2nd Ed., McGraw-Hill, 1979.

Urban, L.A., "Parameter Selection for Multiple Fault Diagnostics of Gas Turbine Engines," AGARD-CP-165, 1974.

Wulf, Ray H., "Engine Diagnostics Program: CF6-50 Engine Performance Deterioration," NASA CR-159867, conducted by the General Electric Company, Aircraft Engine Business Group, 1980.